

Physical properties of CdS:Ga thin films synthesized by spray pyrolysis technique

S. Yılmaz¹ · İ. Polat² · M. A. Olgar³ · M. Tomakin⁴ · S. B. Törelİ⁵ · E. Bacaksız³

Received: 15 August 2016 / Accepted: 17 October 2016 / Published online: 21 October 2016
© Springer Science+Business Media New York 2016

Abstract This paper reports the investigation of physical properties of CdS:Ga thin films grown for the first time by a simple spray pyrolysis method as a function of Ga-doping level from 0 to 8 at.%. X-ray diffraction (XRD), scanning electron microscopy (SEM), energy-dispersive photoelectron spectroscopy, transmittance, photoluminescence, Hall effect and resistivity measurements are utilized to search for the structural, morphological, chemical, optical and electrical properties of as-prepared samples. XRD data confirm the presence of hexagonal structure with a strong (101) preferred orientation. SEM results show that the surface morphology varies significantly via Ga-doping, particularly 6 at.% doping level. Optical transparency is improved by the lower Ga-doping (2 and 4 at.%) whereas higher doping concentration (6 and 8 at.%) causes a poor transmission in the visible region. With respect to CdS (2.42 eV), the calculated band gap values at first enhances for 2 at.% Ga-doping and reaches to 2.43 eV. But, further increase in Ga-doping amount leads to a drop in the band

gap value (2.39 eV) for 8 at.% Ga-doping. Electrical analyses display that 2 at.% Ga-doped CdS thin films exhibit a maximum carrier density and a minimum resistivity that are related to the substitutional incorporation of Ga³⁺ ions at Cd²⁺ ions. However, higher doping of Ga atoms into CdS gives rise to a gradual diminish in the carrier concentration and a rise in the resistivity. Based on all the data, it should be concluded that 2 at.% Ga-doped CdS thin films exhibit the best optical and electrical properties that can be used in the optoelectronic applications.

1 Introduction

CdS is one of the most important semiconductor materials of II-VI group and has a direct band gap value of 2.42 eV at room temperature, with an exciton binding energy of 28 meV. Owing to intrinsic defects including sulphur vacancy (V_s) and interstitial cadmium (I_{Cd}), CdS displays n-type conductivity. n-type CdS has drawn significant attention due to its unique electronic and optoelectronic properties and it is widely utilized in many application areas such as a window layer in CdTe and CuInGaSe₂ solar cells [1, 2], optical sensors [3], photodetectors [4] and field effect transistors [5].

There are a lot of routes that have been used to produce CdS thin films such as sol-gel dip coating [6], chemical bath deposition [7], rf magnetron sputtering [8], laser ablation [9] and spray pyrolysis [10–12]. However, spray pyrolysis is a simple and an inexpensive technique and has also an advantage of large area deposition without using sophisticated equipment. It has been reported that CdS thin films prepared by the spray pyrolysis method have high resistivity and low transmittance values [10]. It is also

✉ S. Yılmaz
slh_yilmaz@yahoo.com.tr

¹ Department of Materials Engineering, Faculty of Engineering and Natural Sciences, Adana Science and Technology University, 01180 Adana, Turkey

² Department of Energy Systems Engineering, Faculty of Technology, Karadeniz Technical University, 61830 Trabzon, Turkey

³ Department of Physics, Faculty of Sciences, Karadeniz Technical University, 61080 Trabzon, Turkey

⁴ Department of Physics, Faculty of Arts and Sciences, Recep Tayyip Erdogan University, Rize, Turkey

⁵ Nanotechnology and Engineering Sciences, Graduate School of Natural and Applied Sciences, Adana Science and Technology University, 01180 Adana, Turkey

known that electrical and optical properties of CdS thin films strongly depend on the growth conditions and it is not easy to produce CdS materials with low resistivity and high transparency by just controlling the growth conditions. Therefore, an effective way to obtain such CdS samples is to dope with an appropriate element. Incorporation of group III elements such as Ga, Al and In into CdS structure could decrease the resistivity by means of substituting of trivalent cations (Ga^{3+} , Al^{3+} and In^{3+}) into Cd^{2+} ions, which can conclude to improve the electrical properties of CdS materials. Additionally, doping of trivalent cations into CdS could also improve the optical properties of CdS materials. Such enhancements in the electrical and optical properties are needed for aforementioned optoelectronic applications. Although the literature consists of many works on Al- and In-doped CdS materials [13–18], the number of reports on Ga-doped CdS thin films is scarce. For example; Ga-doped CdS thin films were grown by Khallaf and co-workers on glass substrates via chemical bath deposition technique. They searched for the influence of Ga atoms on some physical properties of CdS thin film by changing atomic concentration of Ga [19]. Yang et al. produced CdS:Ga sample via solvothermal method using ethyl alcohol and they investigated the photocatalytic performance of the obtained sample in terms of both experimental and theoretical aspects. They found that the incorporation of Ga atoms into CdS enhanced the photocatalytic activity of the samples [20]. Furthermore, Cai and co-workers grew Ga-doped CdS nanowires by thermal evaporation method on silicon substrates to fabricate metal–insulator–semiconductor field-effect transistors (MISFETs) and nano-light emitting diodes (nano-LEDs). They obtained that Ga-doping treatment improved the electrical properties of CdS nanowires and thus the performance of the fabricated devices [21]. Therefore, the motivation of the presented work is to improve the optical and electrical properties of CdS thin films through Ga-doping. To do this, we have altered the atomic concentration of Ga from 0 to 8 at.% in CdS thin films and this is the first report concentrating on Ga-doped CdS thin films prepared by the spray pyrolysis method on glass substrates. We have examined the influences of Ga-doping level on the structural, morphological, optical and electrical properties of CdS thin films in detail.

2 Experiments

CdS and Ga-doped CdS thin films were grown by a homemade spray pyrolysis method on glass substrates. The schematic diagram of the system can be found in elsewhere [22]. Prior to deposition, the glass substrates ($1 \times 1.5 \text{ mm}^2$) were subsequently cleaned in acetone,

ethanol and in distilled water for 10 min by using ultrasonic bath and then dried with air flow. To prepare the CdS solution, 0.05 M cadmium chloride (CdCl_2) and 0.1 M thiourea ($(\text{NH}_2)_2\text{CS}$) were dissolved in distilled water (100 ml). However, besides cadmium chloride and thiourea, gallium nitrate ($\text{Ga}(\text{NO}_3)_3$) salt was used in the solution to obtain Ga-doped CdS samples. The doping level of Ga was changed from 0 to 8 at.% in the solution. The substrate temperature was kept constant at 400 °C and the deposition time was applied for 20 min. The distance between nozzle and substrate was adjusted as 20 cm and the spraying rate was maintained as 2 ml/min using compressed air. Substrate plate was rotated at the speed of 10 rev/min. After the deposition, it was seen that a uniform coverage and a good adherence to the glass substrate surface were accomplished for CdS and Ga-doped CdS thin films.

The structural characterization was performed through X-ray diffraction (XRD) measurements using Rigaku D/Max-IIIC diffractometer with a $\text{CuK}\alpha$ radiation in the range of 20°–60° at room temperature. Morphological and elemental analyses were investigated using a JEOL JSM 6610 scanning electron microscope (SEM) equipped with an energy dispersive of X-ray spectroscopy (EDS) (Oxford Instruments). Transmittance spectra of the samples were recorded using Dongwoo Optron device operating at a Xe lamp with a power of 450 W. The same device was used to take room temperature photoluminescence (RTPL) data with a light source at 400 nm. Electrical characterization was realized at room temperature using Hall effect experiments and four probe method to determine the carrier concentration and resistivity of the samples, respectively.

3 Results and discussion

The crystalline phase and crystallite size of the samples are investigated using XRD data and the results of CdS, 2, 4, 6 and 8 at.% Ga-doped CdS samples are displayed in Fig. 1a–e, respectively. Figure 1a indicates the XRD pattern of CdS sample. The sample exhibits polycrystalline character with the peaks located at 25.0°, 26.7°, 28.4°, 36.7°, 43.9°, 47.9°, 52.0°, 53.0° and 58.5° that are indexed to the reflections of (100), (002), (101), (102), (110), (103), (112), (201) and (202) planes of hexagonal wurtzite structure of CdS (JCPDS card no: 41-1049) with the preferential orientation of (101). As CdS is doped with various levels of Ga atoms, it is seen that there is no change in the preferential orientation. But, as compared to CdS sample, the peak intensity of (101) for CdS:Ga samples increases gradually up to 6 at.% Ga-doping concentration. This situation could be explained by the improvement of the crystal quality. However, further increase in the Ga-

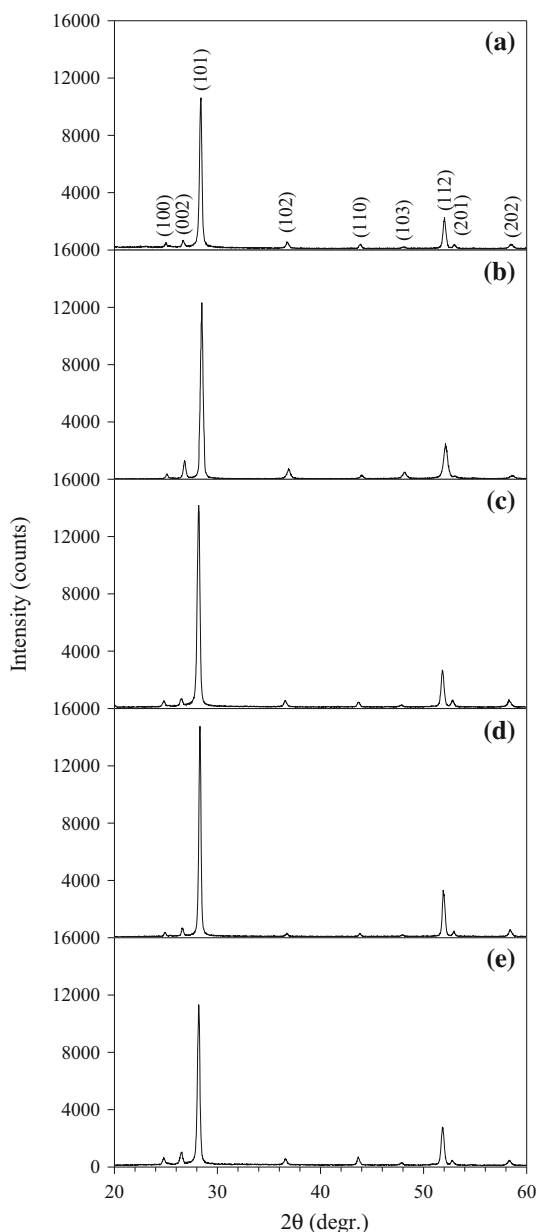


Fig. 1 XRD data of **a** CdS, **b** 2 at.%, **c** 4 at.%, **d** 6 at.% and **e** 8 at.% Ga-doped CdS thin films

doping amount (8 at.%) causes to degrade the crystal quality as Ga atoms occupy interstitial position in the CdS host matrix, concluding more distortion in the volume of unit cell as well as a rise in the population of lattice imperfections. It is known that interstitial incorporation of Ga atoms in CdS gives rise to a deterioration in the crystal structure. Ravichandran and co-workers examined the influence of In-doping on CdS thin films by varying the In doping level from 0 to 8 at.%. They found a reduction in the crystal quality with the increase of In-doping amount up to 8 at.% [16]. No peaks of metallic Ga and secondary phases like GaS and/or Ga₂S₃ are observed in the pattern,

implying that Ga atoms successfully dissolved in the CdS matrix. To determine the lattice parameters (*a* and *c*) of CdS and CdS:Ga samples; (100) and (002) reflection planes are used, respectively. It is listed in Table 1 that CdS sample has *a* value of 0.411 nm and *c* value of 0.668 nm. After 2 at.% Ga-doping, these values decrease to 0.409 and 0.665 nm, respectively, which is an indication of substitutional incorporation of Ga ions in CdS as it is known that Ga³⁺ ions have smaller ionic radius (0.062 nm) than that of Cd²⁺ ions (0.097 nm). Hence, a shrinkage in the volume of unit cell is observed. However, with respect to CdS sample, it is seen from Table 1 that *a* and *c* values increase for the other doping levels (4, 6 and 8 at.% Ga-doping), which imply that Ga ions begin to enter interstitially in the CdS host matrix and thus, an expansion in the volume of unit cell is obtained.

To calculate the average crystallite size of the samples, Scherrer formula [10] is utilized through (101) reflection plane and the results are summarized in Table 1. It can be seen that CdS sample has a *D* value of 31 nm. After various amounts of Ga-doping, there is not seen any big change in the crystallite size values of CdS samples. However, the variation in the crystallite size after and before Ga-doping is similar to the change in the grain size (can be seen below).

In order to obtain knowledge about surface morphology of the produced samples, SEM measurements are recorded and the results are displayed in Fig. 2a–f. Figure 2a indicates the top view image of CdS sample. It is obvious that the sample is composed of irregular shaped grains in different size. Smooth and very compact surface morphology with a good connection are observed. Figure 2b shows the surface topography of 2 at.% Ga-doped CdS thin films. It is seen that compared to CdS sample, the surface morphology changes and worm-like shaped grains appear in the picture. It can be said that the grain size becomes smaller with a smooth surface morphology. Furthermore, uniform and continuous surface morphology without voids appear. As for 4 at.% Ga-doping (Fig. 2c), in addition to worm-like shaped grains, a small amount of undefined shaped grains

Table 1 Lattice parameters and crystallite sizes of CdS, 2, 4, 6 and 8 at.% Ga-doped CdS thin films

Sample	Lattice parameters		Crystallite size <i>D</i> (nm)
	<i>A</i> (nm)	<i>C</i> (nm)	
CdS	0.411	0.668	31
2 at.% Ga-doped CdS	0.409	0.665	28
4 at.% Ga-doped CdS	0.414	0.673	29
6 at.% Ga-doped CdS	0.412	0.671	35
8 at.% Ga-doped CdS	0.415	0.671	30

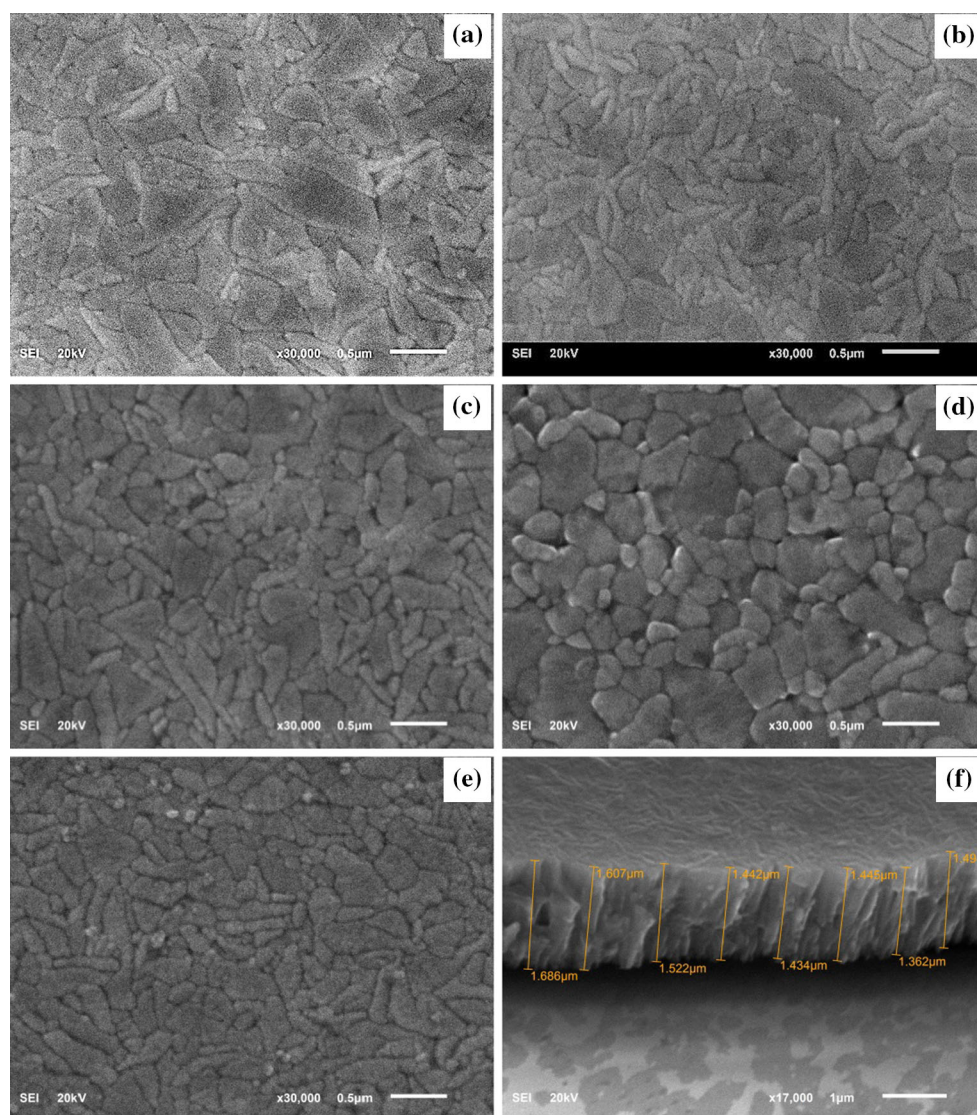


Fig. 2 SEM images of **a** CdS, **b** 2 at.%, **c** 4 at.%, **d** 6 at.% and **e** 8 at.% Ga-doped CdS thin films. **f** indicates 60° tilted view of 4 at.% Ga-doped CdS sample

are also present. As illustrated in Fig. 2d, the surface morphology of 6 at.% Ga-doped CdS thin films significantly varies. It is discernible that the shape of grains starts to round and form well-defined grain boundaries while some big undefined shape grains are also seen. The size of grains grows as well. The reason for the increase of grain size may be attributed to the improvement of the crystal quality, which is consistent with XRD results. Figure 2e indicates the surface morphology of 8 at.% Ga-doped CdS sample. It is clearly seen that this morphology is very similar to that of 2 and 4 at.% Ga-dopings. Additionally, the grains are almost uniformly distributed along the entire surface with a denser structure. The 60° tilted SEM picture of 4 at.% Ga-doped CdS sample is also presented in Fig. 2f. As shown, average thickness of the sample is 1.5 μm and a uniform coverage is also reached. It can be

concluded from SEM results that Ga-doping treatment with various amounts has an important influence on the morphology of CdS thin films.

EDS analysis is utilized to survey the chemical composition of the samples and the resultant data related to CdS, 2, 4, 6 and 8 at.% Ga-doped CdS thin films is presented in Fig. 3 and Table 2. Figure 3 shows the EDS spectrum of 6 at.% Ga-doped CdS thin films, approving the presence of Ga atoms in CdS host matrix without having any impurity atoms. As tabulated in Table 2, the ratio of Cd to S is 0.96 for CdS whereas this ratio decreases for Ga-doped CdS thin films, meaning that less stoichiometric films form after Ga-dopings. Additionally, as seen in Table 2, when the nominal atomic concentrations of Ga in CdS samples increase, the actual atomic concentrations of Ga in CdS matrix also rise. The reason for the rise can be

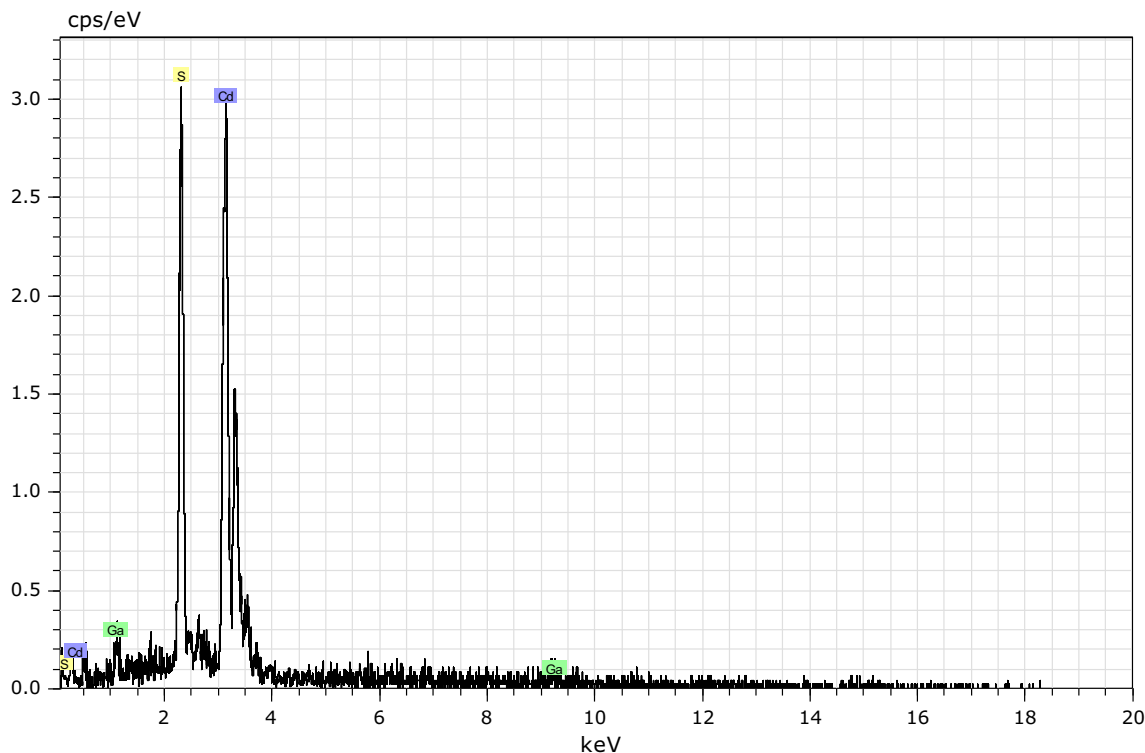


Fig. 3 EDS spectrum of 6 at.% Ga-doped CdS thin films

Table 2 Actual atomic concentrations (at.%) of Cd, S and Ga in CdS and 2, 4, 6, 8 at.% Ga-doped CdS thin films

Samples	Cd	S	Ga
CdS	48.9	51.1	–
2 at.% Ga-doped CdS	46.7	50.6	2.7
4 at.% Ga-doped CdS	46.0	49.1	4.9
6 at.% Ga-doped CdS	45.8	48.7	5.5
8 at.% Ga-doped CdS	43.0	49.0	8.0

attributed to increasing density of Ga atoms in CdS matrix, detected by the EDS measurements.

Optical investigation is made by transmittance and room temperature photoluminescence analyses to survey transmission and defect structure of the samples, respectively. Figure 4 displays the transmittance spectra of CdS, 2, 4, 6 and 8 at.% Ga-doped CdS thin films. As seen, the transmittance values of CdS and CdS:Ga thin films exhibit an increasing trend in the visible region and saturate over 800 nm, reaching the values between 60 and 70 % at 820 nm. In the visible region, compared to CdS sample, transmittance values for 2 and 4 at.% Ga-doped CdS samples rise sequentially and further increase in Ga-doping level up to 6 and 8 at.% give rise a gradual drop in the transparency of the samples. The increase in the transmittance could be ascribed to the improvement in the crystal quality whereas the decline may be commented by the

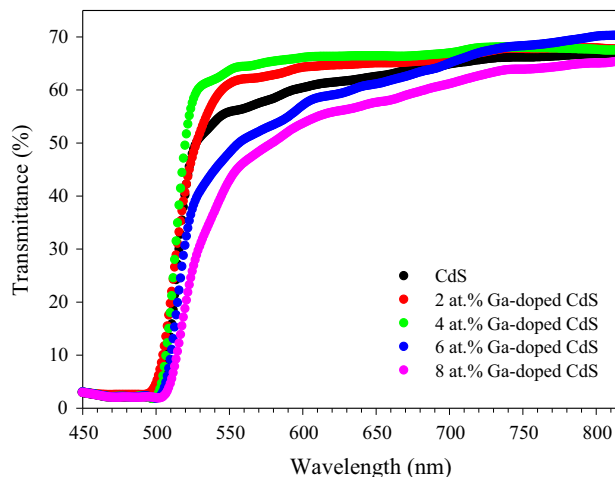


Fig. 4 Transmittance data of CdS, 2, 4, 6 and 8 at.% Ga-doped CdS thin films

crystal defects triggered by the Ga atoms. It can be also stated that 2 at.% Ga-doping causes the absorption edge to shift towards shorter wavelength with respect to CdS sample while the absorption edge consecutively moves towards longer wavelength values at higher doping levels (4, 6 and 8 at.% Ga-doping). The band gap values of the samples are calculated using Tauc’s plot estimation and the resultant data are represented in Fig. 5. As can be seen from the figure, CdS sample has a band gap value of 2.42

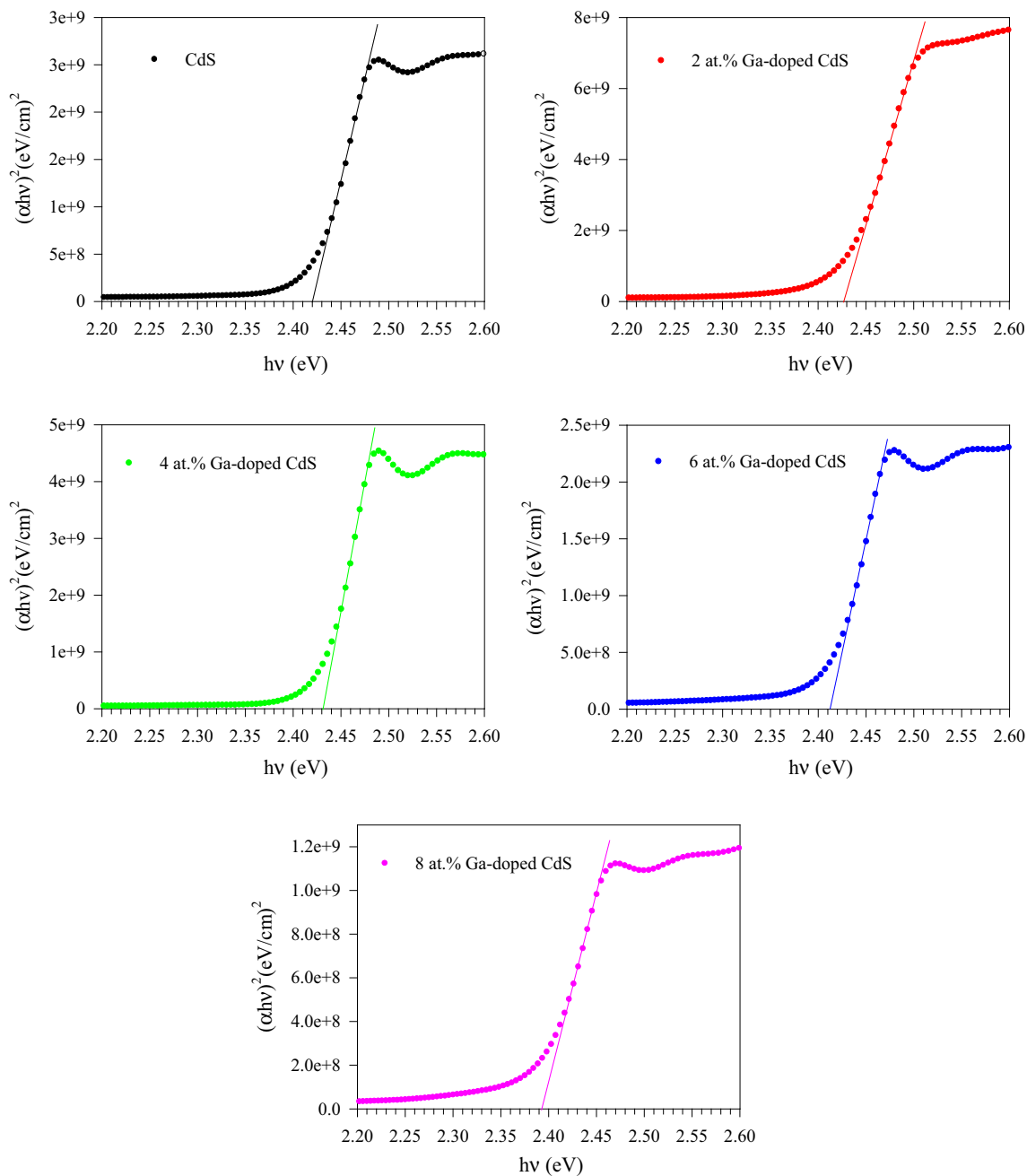


Fig. 5 Tauc's plot results of CdS, 2, 4, 6 and 8 at.% Ga-doped CdS thin films

that is matched well with CdS single crystal. After 2 at.% Ga-doping, the band gap value rises to 2.43 eV, which is referred to Burstein–Moss shift that expresses the band gap broadening due to an increment in the carrier concentration [10]. This result is in good agreement with the XRD data and the result of electrical measurement. That is, XRD data approves that Ga^{3+} ions occupy substitutional position in CdS at sites of Cd^{2+} , resulting in donating a free electron

into host matrix and hence improving the carrier concentration of CdS (will be interpreted later). On the other hand, the band gap value of CdS:Ga (4 at.%) is also 2.43 eV, which is bigger than that of CdS. The reason for this case cannot be attributed to the Burstein–Moss shift as Ga^{3+} ions no longer enter substitutional sites in CdS. Instead, Ga^{3+} ions locate interstitial position in CdS matrix. Thus, an increase in the band gap with respect to CdS could be

explained by the rise of lattice strain because of reduction in the grain size upon 4 at.% Ga-doping as illustrated in Fig. 2a, c [19]. However, the band gap values of 6 and 8 at.% Ga-doped CdS thin films are found to be 2.41 and 2.39 eV, respectively. A similar drop after doping was also reported by Khallaf and co-workers for CdS:Ga thin films [19], Yan and co-workers for CdS:B samples [23] and Akintunde for CdS:Al samples [24]. The fact lies behind the decline is that as Ga^{3+} ions incorporate in the CdS structure, they form donor states in the band gap. Increasing number of Ga atoms in CdS makes these donor levels degenerate and merge into the conduction band of CdS, causing the conduction band to extend into the band gap and hence, a reduction in the band gap takes place [25].

RTPL data of CdS, 2, 4, 6 and 8 at.% Ga-doped CdS thin films are illustrated in Fig. 6. As seen, there are three main peaks in the spectrum of CdS thin films: The first one is located between 480 and 485 nm and the second one is centered in the range of 490–500 nm and the third one is settled between 505 and 675 nm. While the first peak is related to the host CdS, the second one corresponding to green band is ascribed to the excitonic transitions or interstitial sulphur (I_s) vacancies [10, 26]. The last one (called as deep level emission, DLE) exhibits a broad spectrum with an asymmetric shape. Therefore, it includes more than one component associated with intrinsic defects such as cadmium interstitials (I_{Cd}), sulphur vacancies (V_s) and cadmium vacancies (V_{Cd}). After 2 at.% Ga-doping, the spectrum shows almost the same behavior except for the intensity of DLE band that has the lower than that of CdS. The reason for this may be commented by the lesser number of defects, causing an enhancement in the crystal quality (confirmed by XRD data). On the other hand, 4 at.% Ga-doped CdS thin films display the maximum

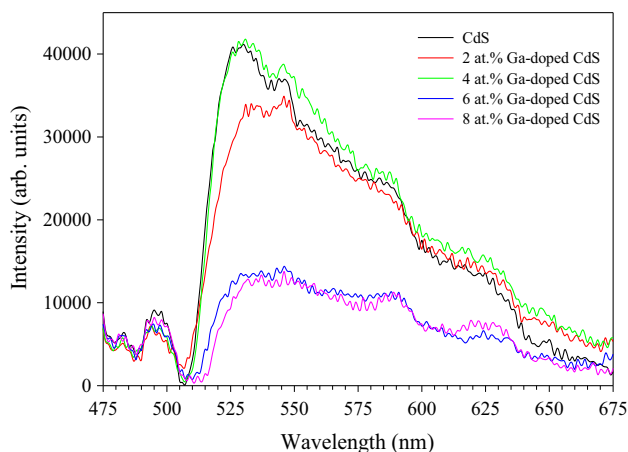


Fig. 6 RTPL data of CdS, 2, 4, 6 and 8 at.% Ga-doped CdS thin films

DLE band intensity. As discussed in XRD section, Ga^{3+} ions occupy interstitial position in CdS structure rather than substitutional one, which increases the number of I_{Cd} defects and hence the peak intensity of DLE. Moreover, Ga atoms that can also play a sensitizer role in CdS structure trigger the radiative recombination phenomenon, which gives rise to an increment in DLE peak intensity [27]. However, further increase in Ga-doping amount up to 6 and 8 at.% causes consequentially a drop in the DLE band intensity that could be the indication of some probable recombinations between I_{Cd} and V_{Cd} defects, resulting in reduction in the population of both type defects as well as in the DLE band intensity because XRD results still show the interstitial incorporation of Ga^{3+} ions in CdS which causes more I_{Cd} defects and EDS results also indicate the existence of more V_{Cd} defects when CdS thin films are doped with 6 and 8 at.% Ga atoms [14]. A similar result was recorded by Muthusamy et al. [13] in their study of CdS:Al thin films where 6 at.% Al-doping brought about a deterioration in the PL intensity.

Electrical properties of the samples are researched by the Hall effect and four probe method to determine the carrier density and resistivity of the samples, respectively and the results are tabulated in Table 3. It can be seen that CdS sample displays in turn a carrier concentration of $6.18 \times 10^{10} \text{ cm}^{-3}$ and a resistivity of $4.14 \times 10^4 \Omega \text{ cm}$. After 2 at.% Ga-doping, the carrier concentration of CdS thin films exhibits the value of $9.91 \times 10^{12} \text{ cm}^{-3}$ that is almost two orders of magnitude higher than that of CdS. This is because Ga^{3+} ions replace Cd^{2+} ions substitutionally rather than interstitially for 2 at.% Ga-doped CdS as discussed in XRD results, which leads to an increase in the population of the free carriers and hence an increment in the carrier density. Furthermore, 2 at.% Ga-doped CdS has the lower resistivity value of $1.53 \times 10^3 \Omega \text{ cm}$ that is smaller than that of CdS. The decline in the resistivity could be clarified by the improvement in the carrier concentration and in the crystal quality as a result of low amount of Ga-doping. However, once CdS thin films are doped separately with 4 and 6 at.% Ga atoms, the carrier concentration starts to reduce and reach to the value of $7.89 \times 10^{10} \text{ cm}^{-3}$ for 6 at.% Ga-doping. This decrease is due to the interstitial incorporation of Ga^{3+} ions in CdS structure (argued previously). As known, interstitially incorporated Ga^{3+} ions in CdS do not behave donors since they are not electrically active. Instead they act as recombination centers, which diminish the carrier concentration. This result is also in a good agreement with the reported studies [19, 24, 25]. On the other hand, it is found that the resistivity values of 4 and 6 at.% Ga-doped CdS thin films are 2.61×10^4 and $3.62 \times 10^4 \Omega \text{ cm}$, respectively. The gradual rise in the resistivity with the increase of Ga-doping level could be attributed to the scattering effects

Table 3 Carrier concentration and resistivity values of CdS, 2, 4, 6 and 8 at.% Ga-doped CdS thin films

Sample	Carrier concentration (cm ⁻³)	Resistivity (Ω cm)
CdS	6.18×10^{10}	4.14×10^4
2 at.% Ga-doped CdS	9.91×10^{12}	1.53×10^3
4 at.% Ga-doped CdS	1.75×10^{11}	2.61×10^4
6 at.% Ga-doped CdS	7.89×10^{10}	3.62×10^4
8 at.% Ga-doped CdS	2.36×10^{10}	4.51×10^4

taking place at the grain boundaries, which leads to an increase at the height of grain boundary potential and hence lowering the conductivity of the samples. As for 8 at.% Ga-doped CdS thin films, while the carrier concentration takes its minimum value of $2.36 \times 10^{10} \text{ cm}^{-3}$, the resistivity value of the sample continues to increase. The reduction in carrier concentration and increase in the resistivity can be commented by the deterioration of the crystal quality as more Ga atoms take into the interstitial position in CdS structure, causing further degradation in the host structure. As known, the interstitial incorporation of Ga atoms in CdS causes a disruption in the crystal quality. Additionally, the increase in the number of Ga atoms in CdS leads to much more interactions between free carriers and scattering processes such as phonon, dislocation, grain boundary and ionized impurity scattering, thus giving rise to a reduction in the mobility [10].

4 Conclusions

CdS and Ga-doped CdS thin films are prepared by a simple spray pyrolysis method on glass substrates. XRD data show that the crystal quality enhances up to 6 at.% Ga-doping. But, 8 at.% Ga-doping causes a decline in the crystal quality. SEM results indicate that CdS sample has an irregular shaped and different sized grain structure. After Ga-doping, the topography of CdS samples changes. It is found that transmittance of CdS is in the range of 60–70 % in the visible region and it improves for 2 and 4 at.% Ga-doping whereas 6 and 8 at.% Ga-doping lead to the worse transparency compared to CdS. According to the Tauc's plot estimation, the band gap value of CdS is 2.42 eV and it firstly increases to 2.43 eV for 2 at.% Ga-doping, which can be attributed to the Burstein–Moss effect and then reduces to 2.39 eV for 8 at.% Ga-doping level. PL data illustrate three main peaks in the spectra (the peaks of host CdS, green band and DLE band). Although the peak intensities of host CdS and green band do not change, DLE peak intensity fluctuates upon various Ga-doping concentrations. As for electrical measurements, it is observed that 2 at.% Ga-doping causes an enhancement in both carrier concentration and resistivity. However, further increase in Ga-doping gives rise to a decline in the carrier

concentration and an increment in the resistivity. As a result, it can be pronounced that 2 at.% Ga-doped CdS sample can be utilized for the solar cell applications due to its good electrical and optical properties.

Acknowledgments The work has been financially supported by the research fund of Adana Science and Technology University under the Project No. MÜHDBF.MLZM.2015-16.

References

1. A. Morales-Acevedo, Sol. Energy **80**, 675 (2006)
2. I. Repins, M.A. Contreras, B. Egaas, C. DeHart, J. Scharf, C.L. Perkins, B. To, R. Noufi, Prog. Photovolt.: Res. Appl. **16**, 235 (2008)
3. S.K. Apte, S.N. Garaje, G.P. Mane, A. Vinu, S.D. Naik, D.P. Amalnerkar, B.B. Kale, Small **7**, 957 (2011)
4. C.Y. Wu, J.S. Jie, L. Wang, Y.Q. Yu, Q.A. Peng, X.W. Zhang, J.J. Cai, H.E. Guo, D. Wu, Y. Jiang, Nanotechnology **21**, 505203 (2010)
5. C. Vossa, S. Subramaniana, C.-H. Chang, J. Appl. Phys. **96**, 5819 (2004)
6. A.A. Ziabari, F.E. Ghodsi, Sol. Energy Mater. Sol. Cells **105**, 249 (2012)
7. S. Hemathangam, G. Thanapathy, S. Muthukumar, J. Mater. Sci.: Mater. Electron. **27**, 6800 (2016)
8. D. Kim, Y. Park, M. Kim, Y. Choi, Y.S. Park, J. Lee, Mater. Res. Bull. **69**, 78 (2015)
9. H. Sakai, T. Tamaru, T. Sumomogi, H. Ezumi, B. Ullrich, Jpn. J. Appl. Phys. **37**, 4149 (1998)
10. S. Yilmaz, Appl. Surf. Sci. **357**, 873 (2015)
11. Z. Zang, X. Zeng, J. Du, M. Wang, X. Tang, Opt. Lett. **41**, 3463 (2016)
12. C. Li, Z. Zang, W. Chen, Z. Hu, X. Tang, W. Hu, K. Sun, X. Liu, W. Chen, Opt. Express **24**, 15071 (2016)
13. M. Muthusamy, S. Muthukumar, M. Ashokkumar, Ceram. Int. **40**, 10657 (2014)
14. S. Yilmaz, Y. Atasoy, M. Tomakin, E. Bacaksız, Superlattices Microstruct. **88**, 299 (2015)
15. H. Khallaf, G. Chai, O. Lupan, L. Chow, S. Park, A. Schulte, J. Phys. D Appl. Phys. **41**, 185304 (2008)
16. K. Ravichandran, V. Senthamilselvi, Appl. Surf. Sci. **270**, 439 (2013)
17. W. Zhou, D. Tang, B. Zou, J. Alloys Compd. **551**, 150 (2013)
18. S.J. Ikhmayies, R.N. Ahmad-Bitar, J. Lumin. **149**, 240 (2014)
19. H. Khallaf, G. Chai, O. Lupan, L. Chow, S. Park, A. Schulte, Appl. Surf. Sci. **255**, 4129 (2009)
20. J. Yang, R. Liu, S. Huang, Y. Shao, Y. Huang, Y. Yu, Catal. Today **224**, 104 (2014)
21. J. Cai, J. Jie, P. Jiang, D. Wu, C. Xie, C. Wu, Z. Wang, Y. Yu, L. Wang, X. Zhang, Q. Peng, Y. Jiang, Phys. Chem. Chem. Phys. **13**, 14663 (2011)

22. E. Bacaksiz, S. Aksu, S. Yilmaz, M. Parlak, M. Altunbaş, Thin Solid Films **518**, 4076 (2010)
23. L.L. Yan, X.B. Wang, X.J. Cai, X.J. Li, J. Alloys Compd. **632**, 450 (2015)
24. J.A. Akintunde, J. Mater. Sci.: Mater. Electron. **11**, 503 (2000)
25. C. Lokhande, S. Pawar, Solid State Commun. **44**, 1137 (1982)
26. K. Kaur, G.S. Lotey, N.K. Verma, J. Mater. Sci.: Mater. Electron. **25**, 2605 (2014)
27. G. Giribabu, G. Murali, D.A. Reddy, C. Liu, R.P. Vijayalakshmi, J. Alloys Compd. **581**, 363 (2013)